RUTGERS
THE STATE UNIVERSITY OF NEW JERSEY

A DEEP LEARNING FRAMEWORK BASED ON DYNAMIC CHANNEL SELECTION FOR EARLY CLASSIFICATION OF LEFT AND RIGHT HAND MOTOR IMAGERY TASKS

Jiazhen Hong
jh1590@scarletmail.rutgers.edu
Advisor: Prof. Laleh Najafizadeh
Integrated Systems & NeuroImaging Lab

Introduction

- Ideal brain-computer interfaces (BCIs) need to be efficient and accurate, demanding for classifiers that can work across subjects while using short duration of electroencephalography (EEG).
- The number of channels as well as selecting the right location of channels play key factors in setting the practicality and the accuracy of the BCI.
- In this study, we present a deep learning framework that employs **dynamic channel selection** to **early classify** left vs right hand motor imagery (MI) tasks.

Methods

The proposed framework (**Fig. 1**) consists of three main stages:

- **Preprocessing**
- **Dynamic channel selection** based on the Davies-Bouldin Index (DBI)
- **CNN-LSTM classifier**

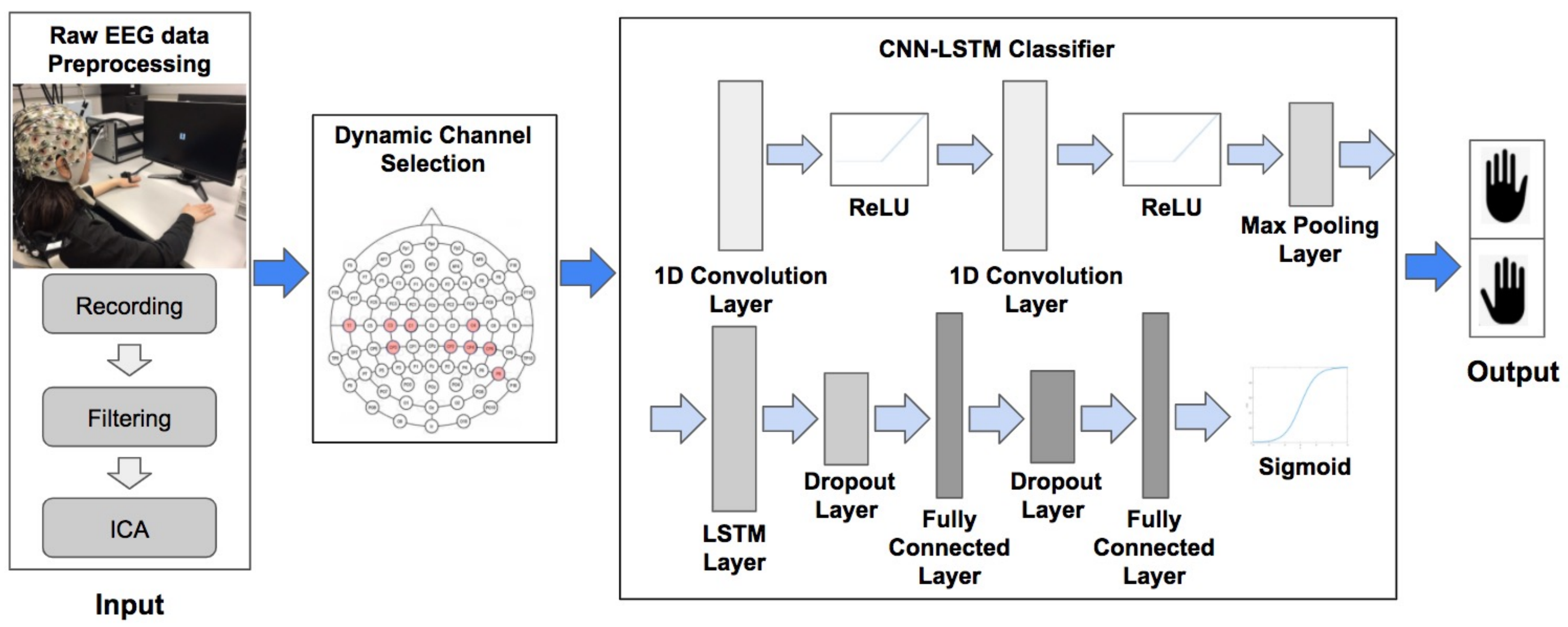

Fig. 1. Overview of the proposed deep learning framework for early classification of left vs right hand MI tasks.

Preprocessing

- The EEG data from each trial is first filtered using a band-pass finite impulse response **(FIR)** filter with the pass-band of [1-50] Hz.
- Artifacts are removed using independent component analysis **(ICA).**

Dynamic Channel Selection

- The DBI is a measure of distinctiveness between two classes of data, and considers both the distance between their centers, and the spreadness of data.
- The DBI is computed as

$$R_{i,j} = \frac{s_i + sj}{\|\mu_i - \mu_j\|}$$

where μ_j and s_j are the center and the spread of the class C_j, respectively. The smaller the $R_{i,j}$, the more significant the contribution of the channel would be in separating the two classes **(Fig. 2).**

Acknowledgement

I want to acknowledge the NSF support for this project.

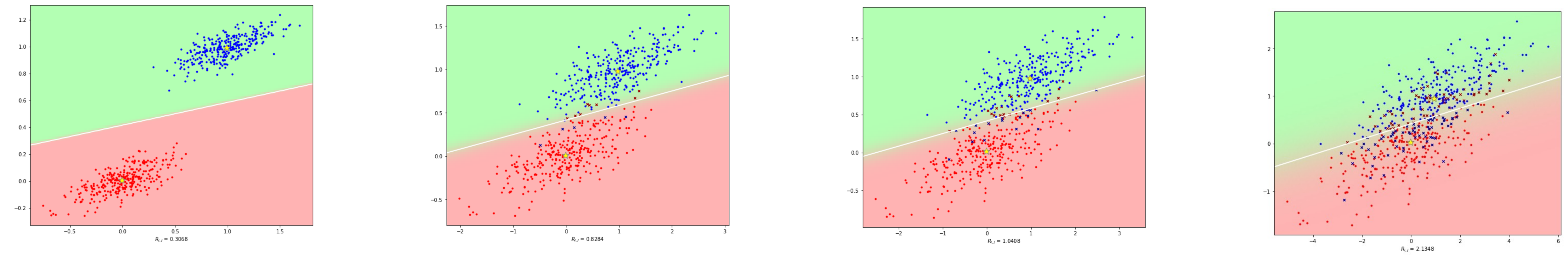

Fig. 2. The overlap degree between two classes, for four different scenarios of various overlaps between classes.

CNN-LSTM Classifier

- The **CNN** contains two 1D convolutional layers, one with 16 filters of size 15, and another with 64 filters of size 64. The second convolutional layer is followed by a max-pooling layer of factor 3.
- The **LSTM** models the temporal dynamics of the extracted by the CNN, in order to avoid the long-term dependency issue that exists in traditional recurrent neural networks.
- Two **fully connected layers** with an output sizes of 64 and 32, activate the abstract features using a sigmoid activation function. A 0.5 dropout layer follows each fully-connected layer.
- Binary cross-entropy is used as loss function. Adam is used as the optimizer.

Results

Channel Selection Strategies

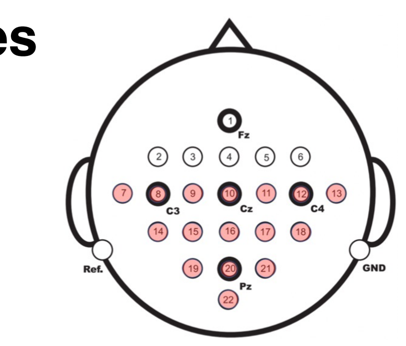

Fig. 3. Location of the electrodes for the **22-chan**. case (shown in black circles) and **16-chan.** case (shown in red).

- **22-chan.:** All available channels
- **16-chan.:** 16 channels close to MI-tasks activities regions [1] **(Fig. 3).**
- **10-chan.:** Top 10 significant channels identified by DBI (fixed number of channels).
- **Dynamic-chan.:** Top significant channels identified by DBI and with $R_{i,j}$ greater than the set threshold. The threshold was set to 11.5 in our setting.

Table 1. Classification accuracy (%) of left and right hand MI tasks for different channel selection methods using 800 ms EEG recording.

Strategies / Subject	22-chan.	16-chan	10-chan.	Dynamic-chan.
A01	49.36	47.27	54.09	55.91
A02	59.09	58.36	59.82	62.73
A03	69.09	70.36	70.91	75.09
A04	64.82	65.18	63.55	67.09
A05	67.09	68.00	70.91	69.09
A06	57.45	62.55	63.18	63.73
A07	62.91	62.00	65.18	65.09
A08	77.27	79.64	71.45	84.73
A09	85.36	86.27	89.73	88.09
Average	65.83	66.74	67.65	70.17

Results

- Comparison of strategies: The **Dynamic-chan.** case reports the best result **(Table 1).**
- Comparison of EEG duration: **1500 ms** reported the best result **(Table 2).**

Table 2. Classification accuracy (%) of left and right hand MI tasks considering dynamic channel selection for various duration after task onset.

Duration / Subject	500 (ms)	1000 (ms)	1500 (ms)	2000 (ms)	2500 (ms)	3000 (ms)
A01	41.09	54.82	58.82	52.09	53.73	56.45
A02	60.27	76.82	71.00	62.91	60.27	58.00
A03	54.82	74.27	82.55	79.36	76.27	68.00
A04	63.09	69.64	72.55	72.64	66.45	64.82
A05	59.18	66.18	73.64	67.18	64.00	66.18
A06	60.91	69.64	78.64	64.91	54.64	57.45
A07	57.45	65.82	64.82	66.36	57.36	58.45
A08	78.64	85.45	90.91	84.91	82.36	72.09
A09	74.18	86.27	92.18	89.55	79.73	77.82
Average	61.07	72.10	76.12	71.10	66.09	64.36

Table 3. Performance comparison with existing works.

Duration / Subject	Ref.	Duration (ms)	Feature	Classifier	Accuracy(%)
2016	[2]	3000	Channel-based	SVM	74.92
2017	[3]	3000	Channel-based	RBM	64.60
2019	[4]	2000	Functional Connectivity	LS	71.00
2021	[5]	800	Functional Connectivity	LSTM	66.27
This paper		800	Dynamic Channel	CNN-LSTM	70.17
This paper		1500	Dynamic Channel	CNN-LSTM	76.18

- It can be concluded that the proposed method is an efficient method for improving the accuracy and efficiency of BCIs for early classification.

References

[1] H. Hamada, et al., "Comparison of brain activity between motor imagery and mental rotation of the hand tasks: a functional magnetic resonance imaging study," Brain Imaging and Behavior, vol. 12, no. 6, p. 1596, 2018.
[2] H. Raza, et al., "Adaptive learning with covariate shift-detection for motor imagery-based brain–computer interface," Soft Computing, vol. 20, no. 8, pp. 3085–3096, 2016.
[3] P. Wang, et al., "LSTM-based EEG classification in motor imagery tasks," IEEE Transactions on Neural Systems and Rehabilitation Engineering, vol. 26, no. 11, pp. 2086–2095, 2018.
[4] P. G. Rodrigues, et al., "Space-time recurrences for functional connectivity evaluation and feature extraction in motor imagery brain-computer interfaces," Medical & Biological Engineering & Computing, vol. 57, no. 8, pp. 1709–1725, 2019.
[5] A. Haddad, et al., "Early decoding of tongue-hand movement from EEG recordings using dynamic functional connectivity graphs," in 9th International IEEE/EMBS Conference on Neural Engineering (NER), 2019, pp. 373–376.